The Indian Geographical Journal
Volume 95 (2) December - 2020, pp. 303-316
ISSN 0019-4824

IMPACT ON CHANNEL PLANFORM CHANGE OF DIKRONG RIVER ON LANDUSE/LAND COVER USING REMOTE SENSING AND GIS

Ranjit Mahato, Rashmita Goswami and Tage Rupa Sora

Department of Geography, Rajiv Gandhi University, Doimukh - 791 112
E-mail: rupa.sora@gmail.com

Abstract

Channel planform of the alluvial river is frequent changes which cause many of the geomorphic hazards due to bank erosion which causes lateral migration of river. The channel planform change and its impact on landuse/ landcover were investigated along a 30.55 Km section of the Dikrong River in Assam for a period of 46 years (1973 to 2019). To determine the channel dynamics, the morphometric characteristics were measured and analyzed by using the Landsat and Sentinel imageries in GIS. The results revealed that the river has gone through a phase of channel straightness (1999-2009) through lateral bank erosion, channel migration and meander cut-off during 1989-1999. As a result, around 24.45 km2 of agricultural and forest area got eroded.

Keywords: *Channel dynamics, Morphometric, Bank erosion, Channel straightness*

Introduction

The implication of rivers in the development of landscapes has always mesmerized geomorphologists, hydrologists, and geologists from a long period of time (Mueller, 1968). The lateral channel shifting, which is adequately rapid on many large rivers, is a geomorphic action, which has the potentiality to generate catastrophic changes in the local and regional level (Hickin, 1983). The people living near the riverbank area always remain vulnerable due to such river actions like changes in the river course and channel morphology (Das et al., 2012)and with the passing of time, some possible human adjustment has been developed to cope up with this nature especially during the flood and bank erosion (Haque, 1988). As the geomorphic phenomena are dynamic in nature, Remote Sensing and Geographical Information System (GIS) has become a standard tool for geo-morphological research (Vitek et al., 1996) because monitoring and observing lateral bank erosion and channel migration through traditional methods and techniques are more time and resource consuming (Bordoloi et al., 2020). In Assam, interest in this field has grown proportionally amongst the researcher of geomorphology, hydrology and earth sciences (Das et al., 2007; Sarkar et al., 2012; Barman and Goswami, 2015; Bordoloi et al., 2020). Though the emergence of geospatial technology has reduced the workload as well

as enhanced the findings of the research, the fieldwork remains a recognized part of doing the geomorphological study.

Though the geomorphic activities like the formation of distributaries, meandering channel, avulsions and confluence migration are common in the rivers of Brahmaputra, the formation, growth, abandonment and reactivation associated with distributaries are dominantly noticeable over the northern tributaries as well as meander dynamics is also frequently visible over the small north bank tributaries (Sah and Das, 2018). Some studies have been done on flood hazard mapping, landslide hazard zonation, morphotectonic evolution, channel changes, soil loss estimation of Dikrong River (Dabral et al., 2007; Pandey et al., 2008; Bhadra et al., 2011; Bezbaruah and Sarma, 2013; Borgohain et al., 2018). The massive erosion along with flash flood during every monsoon season by the Dikrong River has caused great destruction in many parts of its course. Due to which the river has shifted from its usual course and has engulfed most of the agricultural cropland and settlement areas, which has led to the abandonment of villages. The section of 30.55 Km of the river reflects very dynamically related to the channel shifting. The proper study on the nature of bank erosion and its effect has not been carried out properly. Therefore, this kind of study is important to understand the riverine impact on human being and also will help the policymakers to come up with proper planning.

Study Area

The river Dikrong is one of the major tributaries of Subansiri River. The whole catchment area is located between 27°00' N and 27°25' N latitude, and 93°00' E and 94°15' E longitude having an area of 1,556 km^2 where 1,278 km^2 area is situated in Arunachal Pradesh and rest of 278 km^2 situated in Assam (Pandey et al., 2008). After flowing 113 km in Arunachal Pradesh, the Dikrong River entered in Assam plains and flows 32 km long to meet Subansiri River (Bhadra et al., 2011; SJVN Ltd. 2012). Like other north bank tributaries of Brahmaputra, the river Dikrong also facing a steep gradient especially in Arunachal Pradesh with huge sediment load (Borgohain et al., 2018) and receives heavy precipitation during the monsoon period.

Database and Methodology

Data and its Sources

The satellite image of six different years i.e 1973, 1989, 1989, 1999, 2009 and 2019 obtained from United States Geological Survey (USGS). Table 1 presents detail information regarding the applied satellite images.

Data Processing and Analysis

The geo-referenced images are manually digitized to extract the Area of Interest (AOI) and further analysis has been done using the ArcGIS software (version 10.3). The geomorphic correction of Landsat 7 (ETM+) images of 2009 has been performed using the Landsat toolbox. The riverbank erosion and accretion for each side of the banks and shifting of midline channels were measured following the methods of existing literature of Lovric and Tosic (2016) and Deb and Ferreira (2015).

Table 1. Information Regarding Satellite Imageries

Year	Satellite	Sensor	Band Use	Spatial Resolution	Path/Row	Acquisition Date
1973	Lansat 1	MSS	4,5,6,7	60 m	145/41	15-Nov-1973
1978	Lansat 2	MSS	4,5,6,7	60 m	146/41	5-Dec-1978
1989	Lansat 5	TM	1,2,3,4,5,6,7	30 m	135/41	22-Nov-1989
1999	Lansat 7	ETM+	1,2,3,4,5,7	30 m	135/41	25-Oct-1999
2009	Lansat 7	ETM+	1,2,3,4,5,7	30 m	135/41	21-Nov-2009
2019	Sentinel-2A	MSI	2,3,4,8	10 m	-	5-Nov-2019
						15-Nov-2019

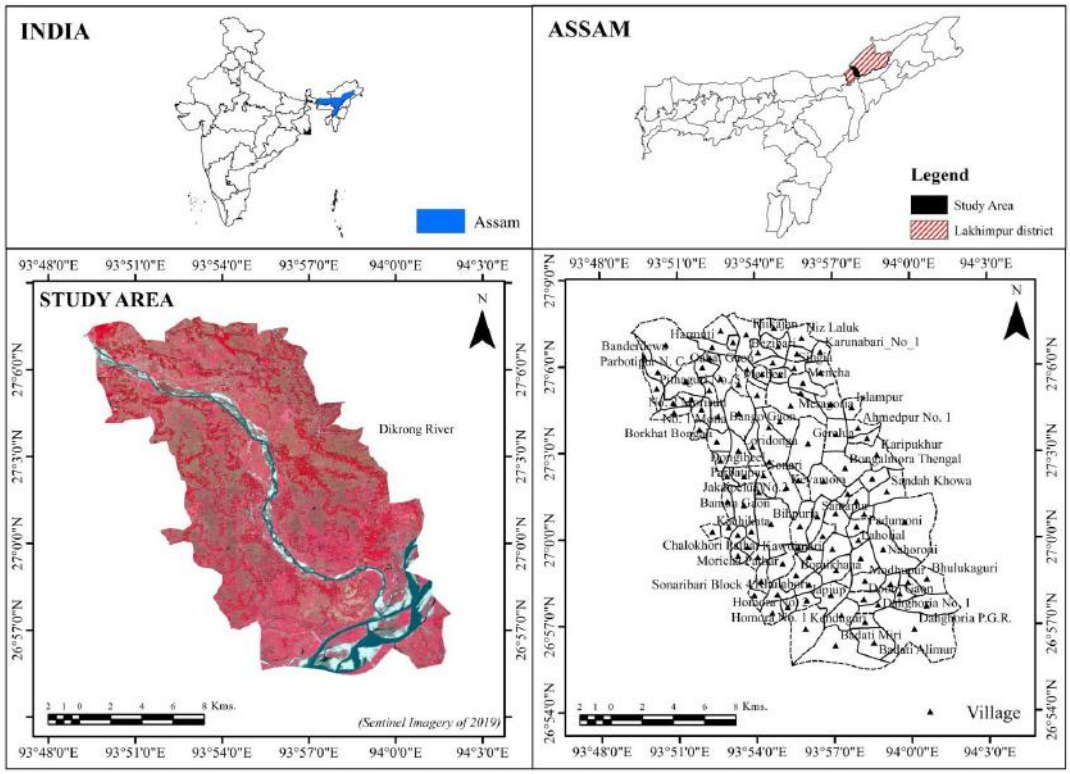

Fig. 1. Location of Study Area

About 38 cross-section lines were considered on the basis of field and visual observation to measure the shifting trend and changing width of the river (Figure 2). The width of the river was measured over every intersection of respective mid-line channel and the cross-section line.

The shifting rates of the channel along the respective cross-sections of a specific time period are measured using the following equation (1)

$$r = \frac{distance\ of mid-line\ channel of\ two\ respective\ time}{No.\ of years\ in\ a\ time\ interval} \quad (1)$$

The mean channel shifting rate during a time interval was measured as per the following equation (2) of Wang et al., (2016) with the alteration of the right bank and left bank:

$$R = \sum_{1}^{n}(a_1 + a_2 + \ldots + a_n)\Big/(n+m) - \sum_{1}^{m}(|b_1| + |b_2| + \cdots + |b_m|)\Big/(n+m) \quad (2)$$

where, '*R*' represents the mean channel shifting rate (metre/year); '*a*' (metre/year, positive) denotes the leftward shifting rate for an intersection point between the mid-channel line and a cross-section; *b* (metre/year, negative) represents the rightward shifting rate for an intersection point between the mid-channel line and a cross-section; '*n*' is the number of the leftward shifted intersection points and '*m*' represents the number of the rightward shifted intersection points; (*n* + *m*) is the total number of the considered cross-sections in a channel. It represents the channel shifted towards left if R is positive, while towards the right when R comes negative. The thalweg length has been measured through the digitizing the centerline of the channel.

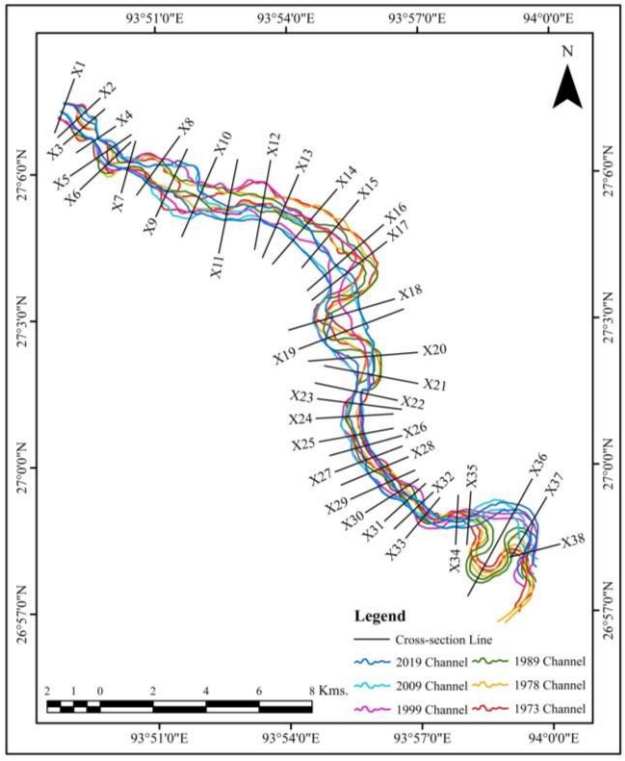

Fig. 2. Cross-Section Line and River Channel of Selected Years

The following equation (3) of sinuosity index (SI), given by Schumm (1963; 1973), has been applied to measure the sinuosity ratio:

SI=(Channel Length)/(Length of the valley) (3)

Results and Discussions

Channel Characteristics

Table (2) reveals an increasing trend of channel length from 1973 to 1989 and a decreasing trend from 1989 to 2019. Accordingly, the thalweg length (line of fastest flow) was increased from 38.37 km. in the year 1973 to 41.78 km. in the year 1989 and thereafter decreased from the year 1989 to 2019 (33.18km.). Similarly, the sinuosity index of the channel increased from 1.43 in the year 1973 to 1.54 in the year 1989 and thereafter decreased to 1.23 in the year 2019.

Table 2. Linear Morphological Characteristics of the Channel

Channel Characteristics	1973	1978	1989	1999	2009	2019
Channel Length (km)	36.00	37.62	38.92	31.54	29.48	30.55
Thalweg Length (km)	38.37	38.84	41.78	32.14	32.89	33.18
Sinuosity Index	1.43	1.47	1.54	1.26	1.19	1.23

Though the sinuosity index (SI) of channels was decreased from 1973 to 2019, an increasing trend of SI was recorded from 1973 to 1989 and a declining trend was recorded from 1989 to 2019 (Table 2). Generally, the declining trend line of SI (R^2=0.645) also represents that the river will become straight in near future (Figure 3).

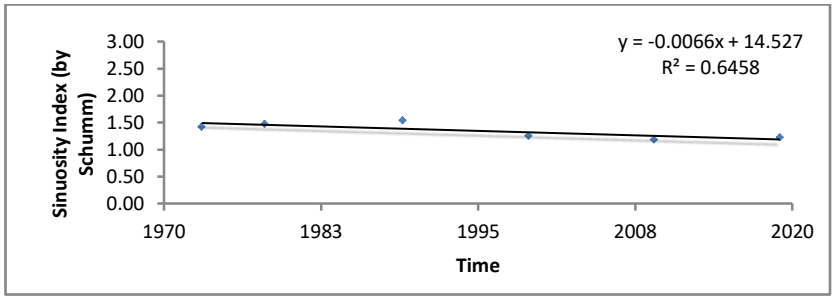

Fig. 3. Variation of sinuosity index with time

Width of the Channel

The channel width reasonably changes within the time period 1973 to 2019 as well as along the channel course (Figure 4). A gigantic change of channel width was recorded over the cross-section X18, X19 and X20, where, the width of the river was increased to 1766.90, 1675.98 and 1124.75 metres respectively in the year 2009 from 374.84, 463.47 and 439.60 metre respectively in the year 1973 with forming an island (0.75 km^2) over the Parbatipur, Gerelua, Keymora and MornoiGaon (Figure 4). Accordingly, in the year 2019, the size of the island increased to 2.30 km^2 but the width was declined to 1083.79, 1553.06

and 820.82 metres respectively. A similar type of changes was also recorded at the cross-section X8, X9 and X10 over the area of Parbatipur No.1 and Pithaguri No.1, where, channel width increased to 1010.18, 1278.02 and 1108.40 metre respectively in the year 1999 from 658.97, 738.28 and 566.70 metres in the year 1973 and further decreased to 759.23, 1220.02 and 802.55 metres respectively in the year 2019 (Figure 4).

Erosion and Accretion along the Riverbank

An area of about 30.506 km^2 suffered bank erosion during 1973 to 2019, where 15.393 km^2 area were eroded from the left bank and 15.112 km^2 area from its right bank (Table 3). Contrary, a total of 27.588 km^2 area accreted during the same time interval where 14.610 km^2 over the left bank and 12.978 km^2 over its right bank (Table 3). The annual yearly rates of erosion were 0.663 km^2 during 1973 to 2019, where, 0.6684, 0.4918, 1.2886, 0.5477 and 0.3391 during the time interval of 1973-1978, 1978-1989, 1989-1999, 1999 to 2009 and 2009-2019 respectively. Accordingly, accretion rate was 0.5997 per year during 1973 to 2019, where, 0.8466, 0.4390, 0.6619, 0.7598 and 0.4309 accreted during the time interval of 1973-1978, 1978-1989, 1989-1999, 1999-2009 and 2009-2019 respectively (Table 4). Generally, the massive erosion and accretion activity was recorded during 1989-1999 and 1999-2009 (Figure 5) where the activity was more prone over the right bank during 1989-1999 and over the left bank during 1999-2009 (Figure 5).

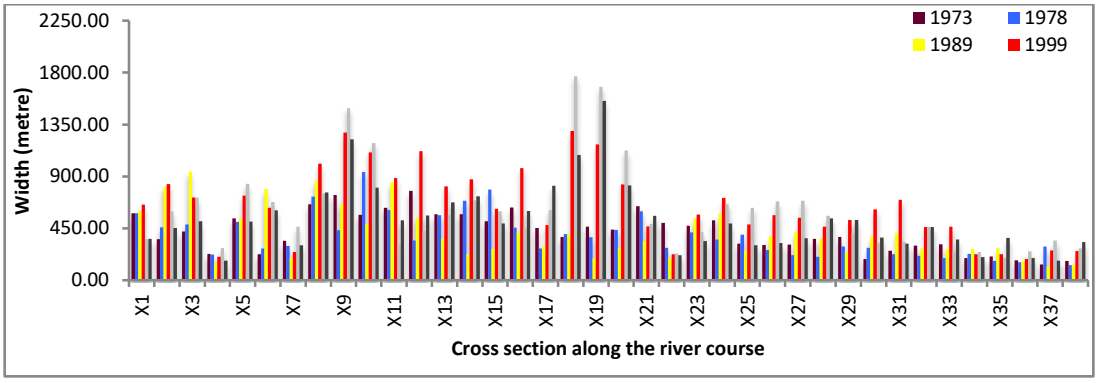

Fig.4. Width of the River Along the Course Section from North to South

Table 3. Area of Riverbank Erosion and Accretion Over the Downstream Dikrong River

Time	Area Where Erosion Occur (km^2)			Area Where Accretion Occur (km^2)		
	Right Bank	Left Bank	Total	Right Bank	Left Bank	Total
1973-1978	1.1487	2.1933	3.3420	2.3580	1.8751	4.2331
1978-1989	2.7079	2.7018	5.4097	2.0688	2.7600	4.8288
1989-1999	6.9502	5.9354	12.8856	3.6336	2.9851	6.6187
1999-2009	2.9000	2.5774	5.4774	1.5157	6.0826	7.5983
2009-2019	1.4057	1.9856	3.3913	3.4018	0.9075	4.3093

Table 4. Rate of Erosion and Deposition

Time	Area Where Erosion Occur (km^2)			Area Where Accretion Occur (km^2)		
	Right Bank	Left Bank	Total	Right Bank	Left Bank	Total
1973-1978	0.0297	0.4387	0.6684	0.4716	0.3750	0.8466
1978-1989	0.2462	0.2456	0.4918	0.1881	0.2509	0.4390
1989-1999	0.6950	0.5935	1.2886	0.3634	0.2985	0.6619
1999-2009	0.2900	0.2577	0.5477	0.1516	0.6083	0.7598
2009-2019	0.1406	0.1986	0.3391	0.3402	0.0908	0.4309
Total	0.3406	0.3220	0.6625	0.2590	0.3106	0.5696

Lateral Channel Shifting

Among the selected 38 cross-sections, 19 cross-sections reflect the leftward shifting of the channel from 1973 to 2019 and the rest of rightward shifting (Figure 6). Although, based on 1973, the river channel of 2019 shifts towards the right due to the higher rate of erosion over the right bank than the left bank (Table 6). During 1973-2019, the highest rightward channel shifts (1350.60 metres with 29.36 $metre^{-1}$) was observed at the cross-section X16, under the area of Bango Gaon and Hoimari No. 79/87 Nlr, where the highest leftward shifting (2600.78 metres with 56.54 $metre^{-1}$) was observed at cross-section X36 of Nahorani village. Similarly, the lowest rightward channel shifting (11.58 metre with 0.25 $metre^{-1}$) and the leftward shifting (41.74 metres with 0.91 $metre^{-1}$) was observed at the cross-section X31 and X32 respectively over the Gondhia Gaon. During the predicted time interval (2019-2024), the mid-channel may shift leftward (Table 5 and Figure 7) where the highest leftward shift (725.34 metres with 145.07 $metre^{-1}$) may observe at the cross-section X17 of Bongalmora Grazing Ground and the rightward shift (1397.45 metres with 279.49 $metre^{-1}$) may visible at the cross-section X36 of Doom Gaon (Table 5 and 6).

Impact Area Assessment

Landuse/landcover (LULC) classification (Figure 8) has been generated using supervised classification with a maximum likelihood algorithm. The overall accuracy assessment were found to be 84.40%, 92.11%, 87.38%, 94.88%, 93.15% and 94.82% for the year 1973, 1978, 1989, 1999, 2009 and 2019 respectively with Kappa Coefficient of 0.7932, 0.8959, 0.8340, 0.9345, 0.9122 and 0.9312. In general, the classified images revealed an increasing trend of agricultural land and built-up area with a decreasing trend of forest cover (Table 7). During the observation period, the highest agricultural area was affected during 1989-1999 with the area of 8.7612 km^2 (0.8761 km^2/year) followed by 2.6741 km^2 (0.2431 km^2/year) during 1978-1989, 2.3661 km^2 (0.2366 km^2/year) during 2009-2019, 1.0784 km^2 (0.2157 km^2/ year) during 1973-1978 and 1.9670 km^2 (0.1967 km^2/year) during 1999-2009 (Table 8).Similarly, the highest forest cover was affected during 1999-2009 with an area of 2.7914 km^2 (0.2791 km^2/year) followed by 1.9102 km^2 (0.1910 km^2/year) during 1989-1999, 1.7522 km^2 (0.1593 km^2/year) during 1978-1989, 0.6187 km^2

(0.1237 km^2/year) during 1973-1978 and 0.5265 km^2 (0.0526 km^2/year) during 2009-2019. Likewise, the predictive channel of 2024 revealed that around 3.9444 km^2 (1.3119 km^2 from the right bank and 2.6325 km^2 from the left bank) of the agricultural area with a rate of 0.7889 km^2 per year and 0.7468 km^2 (0.2891 km^2 from the right bank and 0.4577 km^2 from the left bank) of forest area with a rate of 0.0747 km^2 per year may be affected by the channel migration during the time interval of 2019-2024 (Table 8).

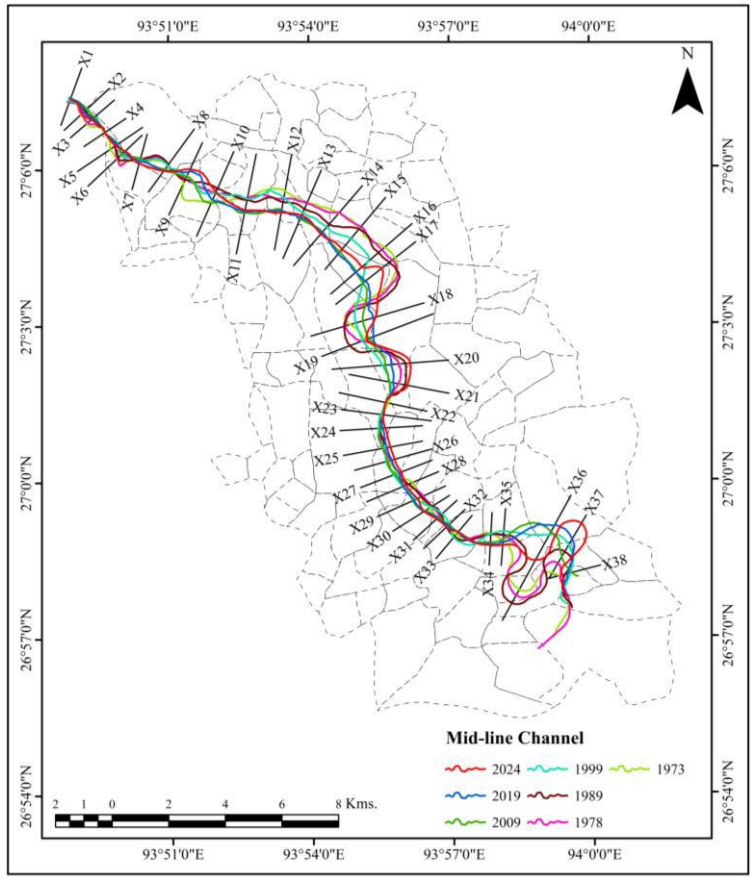

Fig. 5. Shifting of Mid-Line Channel and Future Prediction

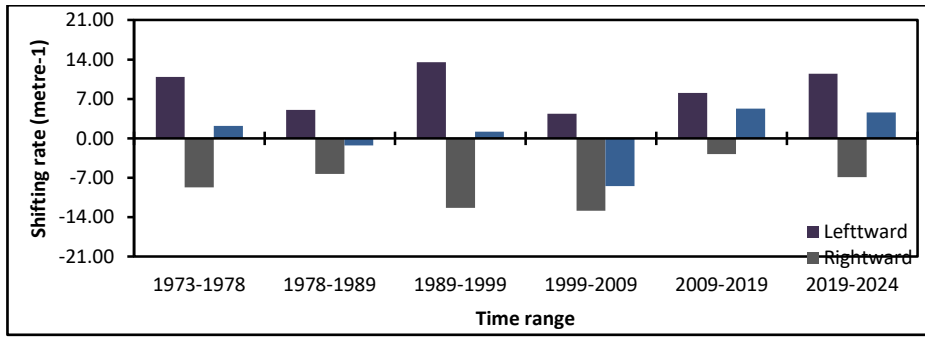

Fig. 6. Average Shifting Rate of the River Channels (metre^{-1})

Table 5. Lateral Channel Sifting and Future Prediction

Channel Shifting Based on the Year 1973					
Cross Section	1978	1989	1999	2009	2019
X1	7.61	41.84	50.63	168.54	142.31
X2	31.17	231.00	302.15	266.96	151.18
X3	42.37	303.44	357.67	355.55	263.19
X4	-14.31	-3.12	-20.46	-8.88	-14.63
X5	181.12	204.35	318.76	307.93	298.20
X6	29.95	73.55	225.90	262.82	379.22
X7	46.09	17.28	11.52	49.83	-40.09
X8	-25.65	7.31	-23.87	-184.89	-250.38
X9	171.35	148.54	295.88	262.58	461.53
X10	312.79	497.30	327.34	-72.01	51.91
X11	13.62	-73.23	-27.28	-536.91	-490.13
X12	-274.18	-397.59	-250.82	-689.78	-703.88
X13	-4.95	-223.91	-360.61	-613.22	-565.37
X14	37.61	-516.92	-645.06	-873.93	-898.64
X15	77.48	-23.78	-477.17	-1071.18	-1169.87
X16	-128.75	-290.76	-802.73	-1328.97	-1350.60
X17	-131.79	-253.18	-1459.20	-1442.39	-1343.39
X18	-172.54	-212.14	196.69	472.35	855.71
X19	-139.19	-584.48	-110.46	139.90	305.04
X20	-25.21	212.28	-610.04	-500.61	-296.82
X21	-18.90	214.26	-318.44	-347.31	-194.57
X22	-92.86	-98.04	-106.79	-92.43	-95.61
X23	-36.46	-56.28	-52.83	55.58	62.25
X24	18.55	73.25	6.15	85.80	143.57
X25	-25.35	-53.68	-42.74	-86.41	62.88
X26	116.38	-16.69	-55.58	-18.52	134.94
X27	83.02	-89.33	-129.02	-69.46	64.21
X28	-168.05	-165.30	-385.33	-350.01	-369.07
X29	78.47	14.25	-178.66	-311.27	-273.45
X30	93.09	120.79	62.99	-183.23	-244.39
X31	100.29	162.86	222.56	39.13	-11.58
X32	-38.63	-23.31	31.74	95.01	41.74
X33	-106.64	-90.99	-137.94	93.38	101.88
X34	-28.34	-34.97	-12.00	-308.22	-373.76
X35	181.38	208.35	340.44	72.38	-26.97
X36	-223.07	-538.56	2216.22	2345.78	2600.78
X37	385.61	864.03	1153.82	661.16	1382.15
X38	66.70	238.40	423.43	466.46	326.00

('+' represents left bank and '-' represents right bank)

Table 6. Rate of Lateral Mid-Line Shifting Between Two Consecutive Years (metre year^{-1})

Cross Section	1973-1978	1978-1989	1989-1999	1999-2009	2009-2019
X1	1.52	3.11	0.88	11.79	-2.62
X2	6.23	18.17	7.11	-3.52	-11.58
X3	8.47	23.73	5.42	-0.21	-9.24
X4	-2.86	1.02	-1.73	1.16	-0.57
X5	36.22	2.11	11.44	-1.08	-0.97
X6	5.99	3.96	15.23	3.69	11.64
X7	9.22	-2.62	-0.58	3.83	-8.99
X8	-5.13	3.00	-3.12	-16.10	-6.55
X9	34.27	-2.07	14.73	-3.33	19.90
X10	62.56	16.77	-17.00	-39.93	12.39
X11	2.72	-7.90	4.60	-50.96	4.68
X12	-54.84	-11.22	14.68	-43.90	-1.41
X13	-0.99	-19.91	-13.67	-25.26	4.79
X14	7.52	-50.41	-12.81	-22.89	-2.47
X15	15.50	-9.21	-45.34	-59.40	-9.87
X16	-25.75	-14.73	-51.20	-52.62	-2.16
X17	-26.36	-11.04	-120.60	1.68	9.90
X18	-34.51	-3.60	40.88	27.57	38.34
X19	-27.84	-40.48	47.40	25.04	16.51
X20	-5.04	21.59	-82.23	10.94	20.38
X21	-3.78	21.20	-53.27	-2.89	15.27
X22	-18.57	-0.47	-0.87	1.44	-0.32
X23	-7.29	-1.80	0.35	10.84	0.67
X24	3.71	4.97	-6.71	7.96	5.78
X25	-5.07	-2.58	1.09	-4.37	14.93
X26	23.28	-12.10	-3.89	3.71	15.35
X27	16.60	-15.67	-3.97	5.96	13.37
X28	-33.61	0.25	-22.00	3.53	-1.91
X29	15.69	-5.84	-19.29	-13.26	3.78
X30	18.62	2.52	-5.78	-24.62	-6.12
X31	20.06	5.69	5.97	-18.34	-5.07
X32	-7.73	1.39	5.51	6.33	-5.33
X33	-21.33	1.42	-4.69	23.13	0.85
X34	-5.67	-0.60	2.30	-29.62	-6.55
X35	36.28	2.45	13.21	-26.81	-9.94
X36	-44.61	-28.68	275.48	12.96	25.50
X37	77.12	43.49	28.98	-49.27	72.10
X38	13.34	15.61	18.50	4.30	-14.05

('+' represents left bank and '-' represents right bank)

Table 7. Landuse/Landcover of the Study Area (in km^2)

Class	1973	1978	1989	1999	2009	2019
Agriculture	117.677	142.656	156.707	129.842	168.657	169.774
Forest	83.753	80.037	61.491	79.983	55.096	45.333
Water	23.763	18.471	17.345	17.815	17.970	15.724
Sand Bank	35.434	19.390	25.042	32.555	18.215	28.563
Built-up	0.242	0.315	0.284	0.674	0.931	1.475

Table 8. Impact Area (in km^2)

Time Range	Agriculture			Forest		
	Right bank	Left bank	Total	Right bank	Left bank	Total
1973-1978	0.4086	0.6698	1.0784	0.2353	0.3834	0.6187
1978-1989	1.5962	1.0779	2.6741	0.5557	1.1965	1.7522
1989-1999	4.7662	3.9950	8.7612	0.9925	0.9177	1.9102
1999-2009	1.2255	0.7415	1.9670	1.2261	1.5653	2.7914
2009-2019	1.0067	1.3594	2.3661	0.1419	0.3846	0.5265

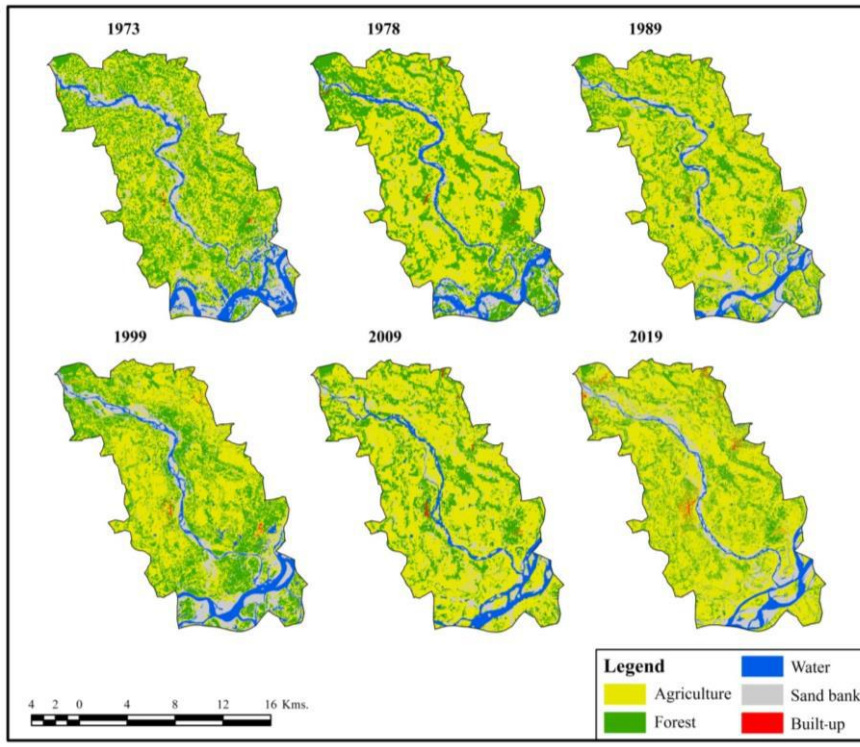

Fig. 7. LULC of the Study Area of Different Time

Various drainage morphological parameters undergo decisive changes due to massive loss to the riverbank areas (Deb and Ferreira, 2015). The mid-line channel and the respective channel width changed dramatically over the time period (1973-2019) owing to the extreme catastrophic events like floods and droughts. The present study revealed that the river Dikrong had undergone channel straightening due to meander cut-offs during the period of 1989-1999 and therefore, a huge amount of erosion and accretion was done during the time interval of 1989-1999. The result also explained by Borgohain et al., 2018 and Sah and Das (2018) where Sah and Das (2018) exposed the meandering cut-off was taken place in upper reach during 1990-1991 and near its confluence in 1993. This process of channel straightening was continued till the period of 1999-2009 where a huge deposition was recorded over the left bank. The lowest channel length (29.48 km) was recorded in 2009 which may be due to the floods of 2004 which further reduced channel length and altered the confluence with the Subansiri River. The river demonstrates a noticeable decrease in sinuosity index. However, the river has a narrower channel than its valley size, the present study found an increasing trend of the horizontal size of the active channel during the time interval of 1973-2019. During 1973-2019, a massive channel shifting occurred over the two parts of the channel. The part one was situated at the cross-section from X10 to X20 and part two was situated at the cross-section from X35 to X38. During this process of channel shifting, part one area gradually affected the villages of Parbatipur No. 1, Merbeel Gt. No. 81/78, MerbeelDighali, Pithaguri No. 5, Merbeel, Holmari Grant No. 65/68, Holmari No. 79/87 Nlr, Bongalmara Grazing Ground, Bongo Gaon, Parbatipur, Gerelua and MornoiGaon. Likewise, part two affected the villages of Pokadol Grant, Modhupur, Doom Gaon, Nahoroni, Madhupur No. 2, Dahghoria No. 1, Dahghoria Block and Dahghoria No. 2. During 1973-2019, the channel shifting has affected an area of around 24.45 km^2 of agricultural and forest area. Due to lateral migration of the channel, a huge portion of inhabitants is facing various problems related to land degradation and land loss. Along with the land loss, the inhabitants living over the confluence zone where the channel migration remains more vulnerable are also facing a huge problem of the flood, especially during the monsoon period.

Conclusion

In the present study, the bank erosions and resultant channel dynamics of the Dikrong river were studied using geospatial techniques. The analysis of remote sensing data for the period of 46 years (1973-2019) indicates a spatial and temporal variation in bank erosion and channel migration. During the time span of 1973-2019, around 24.45 km^2 of agricultural and forest area got eroded due to lateral channel migration. The partial observation over riverbank erosion and channel migration of different time interval reveals that the river is moving towards the west with an intention of channel straightness. The predictive assessment of riverbank erosion using a non-linear regression model represents a satisfactory result and highlights an area of around 4.69 km^2 of agriculture and forest cover may lose due to bank erosion. Besides, the study also exhibits the potential of Remote Sensing and GIS for immediate assessment of bank erosion and channel migration. Thus, the study can be applied for the concerned authority to take suitable mitigation measures and helps to prepare for river management strategies in future.

References

1. Akhter, S., Eibek, K. U., Islam, S., Islam, A. R. M. T., Chu, R., and Shuanghe, S. (2019). Predicting spatiotemporal changes of channel morphology in the reach of Teesta River, Bangladesh using GIS and ARIMA modeling. Quaternary International, 513, 80-94.
2. Barman, P., and Goswami, D. C. (2015). Evaluation of Sinuosity Index of Dhansiri (South) River Channel and Bank Erosion, Assam in GIS. International Advanced Research Journal in Science, Engineering and Technology, 2(5), 111-114.
3. Bezbaruah, D., and Sarma, M. (2013). Morphotectonic Evolution of the Area in and Around Bandardewa, Papumpare District, Arunachal Pradesh. Journal of Earth Science, Special Volume, 223-232.
4. Bhadra, A., Choudhury, S., and Kar, D. (2011). Flood hazard mapping in Dikrong basin of Arunachal Pradesh (India). World Academy of Science, Engineering and Technology, 60, 1614-1619.
5. Bordoloi, K., Nikam, B. R., Srivastav, S. K., and Sahariah, D. (2020). Assessment of riverbank erosion and erosion probability using geospatial approach: a case study of the Subansiri River, Assam, India. Applied Geomatics, 1-16.
6. Borgohain, P. L., Phukan, S., and Ahuja, D. R. (2018). Downstream channel changes and the likely impacts of flow augmentation by a hydropower project in River Dikrong, India. International Journal of River Basin Management, 17(1), 25-35. DOI:10.1080/15715124.2018.1439497
7. Brice, J.C., (1964). Channel Patterns and Terraces of the Loup Rivers in Nebraska. U.S. Geological Survey professional paper 422–D, pp. 41.
8. Dabral, P. P., Pandey, A., and Debbarma, S. (2007). Soil loss estimation of the Dikrong River Basin using IRS-1B LISS II satellite data and GIS. IE (I) Journal-AG, 88, 44-51.
9. Das, A. K., Sah, R. K., and Hazarika, N. (2012). Bankline change and the facets of riverine hazards in the floodplain of Subansiri–Ranganadi Doab, Brahmaputra Valley, India. Natural hazards, 64(2), 1015-1028.
10. Das, B., Mondal, M., and Das, A. (2012). Monitoring of bank line erosion of River Ganga, Maida District, and West Bengal: Using RS and GIS compiled with statistical techniques. International Journal of Geomatics and Geosciences, 3(1), 239-248.
11. Das, J. D., Dutta, T., and Saraf, A. K. (2007). Remote sensing and GIS application in change detection of the Barak river channel, NE India. Journal of the Indian Society of Remote Sensing, 35(4), 301-312.
12. Deb, M., and Ferreira, C. (2015). Planform channel dynamics and bank migration hazard assessment of a highly sinuous river in the north-eastern zone of Bangladesh. Environmental Earth Sciences, 73(10), 6613-6623.
13. Haque, C. E. (1988). Human adjustments to river bank erosion hazard in the Jamuna floodplain, Bangladesh. Human Ecology, 16(4), 421-437.
14. Hickin, E. J. (1983). River channel changes: retrospect and prospect. Modern and ancient fluvial systems, 59-83.
15. Huda, E. A. (2017). Morphometric characteristics of Dikrong River catchment in the foot-hills of Arunachal Himalayas. IOSR Journal of Humanities and Social Science, 22(7), 51-60.
16. Kaliraj, S., Chandrasekar, N., Magesh, N.S., 2015. Morphometric analysis of the River Thamirabarani sub-basin in Kanyakumari District, South west coast of Tamil Nadu, India, using remote sensing and GIS. Environmental Earth Sciences 73, 7375–7401.

17. Lovric, N., and Tosic, R. (2016). Assessment of bank erosion, accretion and channel shifting using remote sensing and GIS: case study–lower course of the bosna river. Quaestiones Geographicae, 35(1), 81-92.
18. Mueller, J. E., (1968). An introduction to the Hydraulic and Topographic Sinuosity Indexes, Annals of the Association of American Geographers, 58(2), 371-385, DOI: 10.1111/j.1467-8306.1968.tb00650.x
19. Pandey, A., Dabral, P. P., Chowdary, V. M., and Yadav, N. K. (2008). Landslide hazard zonation using remote sensing and GIS: a case study of Dikrong river basin, Arunachal Pradesh, India. Environmental geology, 54(7), 1517-1529.
20. Richard, G. A., Julien, P. Y., and Baird, D. C. (2005). Statistical analysis of lateral migration of the Rio Grande, New Mexico. Geomorphology, 71(1-2), 139-155.
21. Sah, R. K., and Das, A. K. (2018). Morphological Dynamics of the Rivers of Brahmaputra. Journal of the Geological Society of India, 92(4), 441-448.
22. Sarkar, A., Garg, R. D., and Sharma, N. (2012). RS-GIS based assessment of river dynamics of Brahmaputra River in India. Journal of Water Resource and Protection, 4(2), 63-72.
23. Schumm, S. A. (1963). Sinuosity of alluvial rivers on the Great Plains. Geological Society of America Bulletin, 74(9), 1089-1100.
24. Schumm, S. A. (1973). Geomorphic thresholds and complex response of drainage systems. Fluvial geomorphology, 6, 69-85.
25. SJVN Limited, 2012. Doimukh Hydro-Electric Project, Arunachal Pradesh. Pre-Feasibility Report. Shimla, India. Available from
26. Vitek, J. D., Giardino, J. R., and Fitzgerald, J. W. (1996). Mapping geomorphology: A journey from paper maps, through computer mapping to GIS and Virtual Reality. Geomorphology, 16(3), 233-249.
27. Wang, S., Li, L., Ran, L., and Yan, Y. (2016). Spatial and temporal variations of channel lateral migration rates in the Inner Mongolian reach of the upper Yellow River. Environmental Earth Sciences, 75(18), 1255.